



LIFE CYCLE VULNERABILITY ASSESSMENT OF MASONRY INFILLED STEEL FRAME STRUCTURES

A. Nassirpour⁽¹⁾, D. D'Ayala⁽²⁾

⁽¹⁾ PhD Candidate, University College London – EPICentre, London-UK, a.nassirpour@ucl.ac.uk

⁽²⁾ Professor of Structural Eng., University College London – EPICentre, London-UK, d.dayala@ucl.ac.uk

Abstract

In this study, the anticipated cost throughout a structure's operational period has been estimated, following a life cycle model. A scenario has been defined in order to assess the structural performance of a mid-rise infilled steel frame over its expected lifetime. Since the characteristics of the index building play a critical role in estimating the losses, the one selected is designed and modelled based on common existing residential buildings. The life cycle cost of the index building has been estimated by considering progressive deterioration due to aging of the structure (e.g. corrosion, fatigue) and also cumulative damage caused by extreme sudden events (e.g. earthquake, hurricane, flood, blast, etc.). The adapted model is capable of considering the initial construction cost along with the cost of damage and failure consequences including death and injuries, as well as discounting cost over time. The performance of the index building at different life stages has been assessed by implementing incremental dynamic analysis (IDA). Using the obtained results, the exceedance probabilities required for the cost analysis are calculated by means of fragility curves for multiple damage limit states. Furthermore, the limit states' exceedance frequencies are obtained by convolving fragilities with site a specific hazard curve. Having a good understanding of the structural behavior and its expected cost forecast can be beneficial as a decision making tool for planning and allocating financial resources in case of both pre- and post- disaster.

Keywords: Life Cycle Cost; Masonry Infilled Steel Frame; Incremental Dynamic Analysis (IDA); Fragility Curve; Vulnerability

1. Introduction

Steel framed structures, with unreinforced masonry infill panels, make up a considerable proportion of residential buildings in seismically active regions (e.g. Japan, China, Turkey, Iran, California) as well as a substantial amount of the world's governmental and public buildings. Due to the interaction of the unreinforced masonry infill and its surrounding frame, when subjected to strong earthquake loads, these structures are at high risk of heavy damage. Thus, such structures can be among the dominant causes of structural failure and casualty.

The seismic loss estimation and vulnerability are greatly influenced by the failure mechanism of the structures. In case of infilled structures, the final failure mechanism differs to that expected during the design and analysis of the structure, mainly due to the resultant composite behaviour of the frame and the infill. Having a rational prediction of the structural deterioration and its consequential cost at each stage of building's operational life can assist in managing and allocation of financial resources, intended for repair, replacement or redesign and reconstruction activities. Furthermore, the outcome of this assessment can lead to cost-effective structural designs, particularly in regions prone to extreme events.

The deterioration of a structure can be summarised as the reduction in performance, reliability and life span of the building. The vulnerability of structures can vary with time and accumulated damage, mainly due to two factors; first is the continues degradation of material characteristics due to aging and environmental factors and second is the accumulation of damage after repeated overloading due to any sudden extreme event (e.g. seismic excitation, hurricane, flood, blast) [1]. In general, the load uncertainties can be related to occurrence, time, intensity and duration. Furthermore, the material property and the strength degradation of structural members are mainly case sensitive and can be related to construction quality and practice.

Structural life cycle cost (LCC) models tend to predict the performance of buildings, infrastructures or components throughout their lifetime of operation. The structural performance in this case is mainly related to deterioration, either progressive degradation or extreme sudden events, and is commonly measured in terms of physical parameters. For instance, parameters such as overall capacity, stiffness, top drift or inter-storey drift are acceptable measures of deterioration in structures. The progressive deterioration is mostly a slow and continuous time dependent phenomenon, which may cause an increase in the seismic structural fragility. Several factors can cause and affect the rapidity of capacity loss in this case, for example corrosion, fatigue or bio-deterioration [2-3]. The damage caused by either of motives will accumulate with time, effecting the material strength and/or the geometric properties, causing a gradual drop in the overall capacity of the structure and its remaining life. A sudden drop of capacity is also feasible and is usually caused due to any unpredictable type of extreme event. A simplified lifetime of a structure, while considering both deterioration elements is illustrated in Fig. 1.

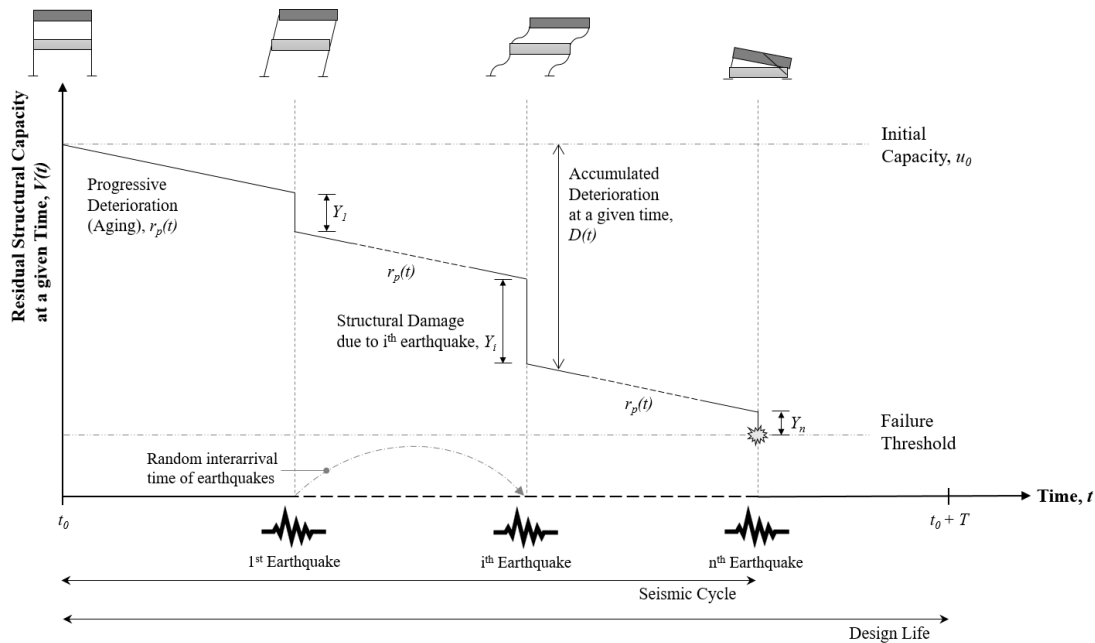


Fig. 1 – Design life of a structure subjected to progressive deterioration (aging) and multiple earthquakes

Looking at a building throughout its operating lifetime has the benefit of delivering effective rehabilitation and reconstruction measures. Having a rational prediction of the structure’s status at various intervals in terms of capacity, ductility, etc., gives the opportunity of comparing the situation with pre-defined thresholds. These thresholds can be defined in a way to indicate whether the structure can still be operational once a sudden incident has occurred or even after a certain period has passed from the life of the building and deterioration has reached a particular point. Accordingly, different levels of preventive intervention or structural repair can be applied. Generally, maintenance programs are based on early repairs, meaning they are carried out prior reaching extensive or complete collapse stages. For instance, in case the structure’s capacity drops below collapse, the only option is to replace the structure, while if the capacity is between extensive damage and collapse thresholds, then preventive maintenance can be carried out to raise back the capacity near to its initial situation and the process starts over. Also, in case the capacity remains higher than the extensive damage, no maintenance is necessary.

Furthermore, in most cases downtime is an important issue and can significantly vary depending on whether the whole building needs to be reconstructed or certain levels of intervention (e.g. repair, retrofit) are necessary. This brings more uncertainty to the life cycle analysis of the buildings. In case of residential buildings, the intervention time is usually shorter compared to the total life of the structure. For sure, this directly depends on the availability of resources, either financial or tools and material. Hence, due to great number of involved factors and the high uncertainty with maintenance process, most life cycle models consider the repair to be instantaneous and without any delay. Thus, the cyclic process of operation, failure and immediate repair can be modelled as a counting process.



The main aim of this study is to estimate the life cycle cost of a mid-rise (4-storey) dual system infilled steel frame structure. Initially, the structural degradation caused by both forms of progressive deterioration and occurrence of sudden earthquake shocks is discussed, followed by a brief review on the probabilistic assessment of seismic hazard and fragility analysis. A scenario is then defined for the 50-year life span of the index building, which includes different deterioration factors. The correlation between possible loss of capacity and the structural response is quantified by means of incremental dynamic analysis (IDA) at three critical stages of the structure's life span. Multiple limit states, based on maximum inter-storey drift ratio are considered for deriving the fragility curves at different stages of the structure's operational life. Furthermore, depending on characteristics of the structure, the exceedance frequencies of the limit-states are obtained by convolving fragilities with corresponding hazard curves. Finally, the expected life cycle cost is estimated by deriving the limit-state dependent costs throughout the structure's life.

2. Structural Deterioration

Over the last two decades, several studies have discussed the life cycle analysis of various structures and different analytical solutions have been proposed [4-7]. Most approaches consider a stochastic model with point process approach to study the time-dependent performance of the building. The proposed models are able to approximate the average capacity loss and the remaining life of the structure, up to a certain time and compare it to specific damage thresholds for further decision making. The following will discuss a generalised life cycle model according to the proposed methods.

The initial capacity of the structure decays as it goes through both progressive and sudden deterioration (e.g. earthquake shock). If the initial capacity of the structure is presented by u_0 and the accumulated capacity drop is shown with $D(t)$ then the residual capacity of structure at time t can simply be defined as:

$$V(t) = u_0 - D(t) \quad (1)$$

This accumulated capacity loss, caused by both progressive deterioration and sudden extreme events, which are completely independent can be expressed as:

$$D(t) = \int_0^t r_p(t)dt + \sum_{i=1}^{N_t} Y_i \quad (2)$$

where $r_p(t)$ simulates the continuous progressive deterioration process due to aging, N_t is the total number of earthquake events up to time t and Y_i is the capacity loss due to earthquake shaking event i . The accumulated seismic damage is defined by summing up the damage caused by every single and independent occurrence of shaking. If this damage is assumed to be exponentially distributed, then the resultant accumulated damage after a certain number of shocks follows an Erlang distribution [17]. Therefore, the residual capacity of the structure by time t can be rearranged as follows:

$$V(t) = u_0 - \int_0^t r_p(t)dt + \sum_{i=1}^{N_t} Y_i \quad (3)$$

In cases which the deterioration due to progressive aging is not considered and the capacity loss is solely due to earthquake shocks, the term $r_p(t)$ is considered equal to zero. Thus, the solution depends solely on the number of shocks and the initial capacity of the structure under study. However, in real life situation, it is common to observe progressive deterioration along with earthquake deterioration. If only the earthquake damage is considered during the lifetime of the building, then the possibility of capacity loss in between shocks will be completely ignored and unrealistic. The progressive deterioration can be modelled by a continuous deterministic function, linear or exponential. Fig. 2 compares different possible model for progressive deterioration with one which does not reflect the deterioration due to time. Fig. 3 illustrates the structural performance, while combining the effects of progressive capacity drop and multiple sudden decays due to extreme events. It is clear that the exponential deterministic function, representing the aging of the structure, stands between over- and under-estimating the time, in which the failure threshold is reached.

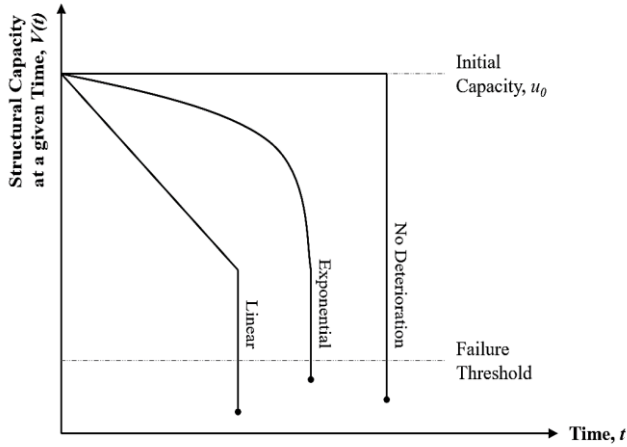


Fig. 2 – Capacity deterioration due to single hazard [1]

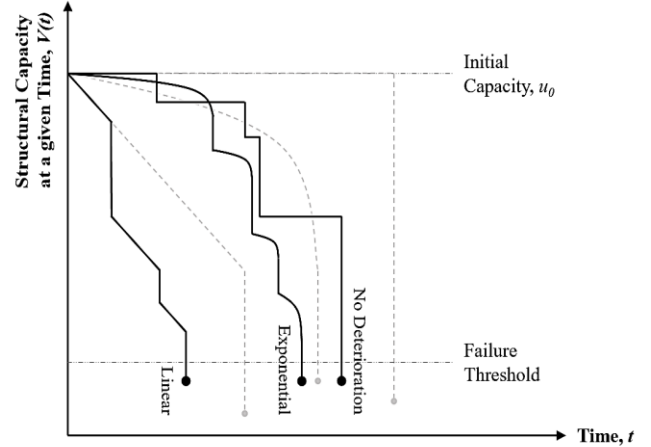


Fig. 3 – Capacity deterioration due to multiple hazards [1]

3. Probabilistic Seismic Assessment

Extreme natural events, such as earthquakes, which have potential to cause considerable damage to structures, are unpredictable and happen randomly in time. Due to the history dependency of earthquake hazards and also independency of sources contributing to the hazard, the arrival of earthquakes can be approximated by stochastic models. In probabilistic seismic hazard assessment (PSHA) the occurrence of seismic events is described via a homogeneous Poisson process (HPP), in which the events are independent with stationary increments (i.e. memory less) and entirely described by one parameter, the occurrence rate ν_E [8].

Accordingly, the probability of any number of seismic events N_E , occurring (e.g. 2 earthquake events) in a defined time interval ΔT (e.g. 50 years) is independent of the history of earthquakes which has happened in the past and can be expressed by a Poisson probability mass function. As a result of the HPP, the inter-arrival time (i.e. time between each arrival into the system and the next; 1/arrival rate) distribution of earthquake events is explained by an exponential distribution of parameter ν_E as follows:

$$P[N_E(t, t + \Delta T) = n] = P[N_E(\Delta T) = n] = \frac{(\nu_E \cdot \Delta T)^n}{n!} \cdot e^{-\nu_E \cdot \Delta T} \quad (4)$$

where n shows the number of shocks happening in a considered time interval (ΔT) with an arrival rate of $\nu_E = 1/\text{year}$.

In probabilistic seismic hazard assessment, the exceedance of an intensity measure (IM) threshold im at a site of interest can also be described by HPP. The intensity or hazard rate $\lambda_{im,E}$ is obtained from ν_E as follows:

$$\lambda_{im,E} = \nu_E \cdot \int_{r_{E,min}}^{r_{E,max}} \int_{m_{E,min}}^{m_{E,max}} P[IM > im | x, y] \cdot f_{M_E, R_E}(x, y) \cdot dx \cdot dy \quad (5)$$

where the term $P[IM > im | x, y]$ is estimated using a ground motion prediction equation (GMPE), representing the probability of exceeding the intensity threshold, given an earthquake of magnitude $M_E = x$ and a separation distance of $R_E = y$. In addition, f_{M_E, R_E} is the joint probability density function (PDF) of the earthquake magnitude and distance random variables. In case these two can be considered independent, f_{M_E} can be obtained from Gutenberg-Richter relationship and f_{R_E} depends on the source-site configuration. In this study, subsequent to the location of the selected index building, the earthquake occurrence will be estimated from the available PSHA studies.

In order to implement the LCC model, the annual probability of exceeding a limit state considering the earthquake intensity is required. The annual frequency of exceeding a maximum response quantity threshold Δ_i is represented by $P_i(\Delta > \Delta_i)$, which is a product of risk analysis:

$$P_i(\Delta > \Delta_i) = \sum_{all\ x_i} P(DS \geq ds_i | IM = x_i) \cdot |\Delta\lambda_{IM}(x_i)| \tag{6}$$

where $\lambda_{IM}(x_i)$ is the annual frequency of exceeding a given intensity measure value x_i (i.e. ground motion hazard) and $|\Delta\lambda_{IM}(x_i)| = |\lambda_{IM}(x_i) - \lambda_{IM}(x_{i+1})|$ is approximately the annual frequency of intensity measure being equal to $IM = x_i$. The $P(DS > ds_i | IM = x_i)$ represents the probability of exceeding a specific damage state limit (ds_i) given the level of seismic intensity (x_i), which is obtained from the fragility function estimation. The derivation process of fragility functions and annual probability of exceeding a limit state, for the building under study has been discussed thoroughly in coming sections.

4. Index Building

4.1 Numerical Modelling

A mid-rise, four storeys residential building has been chosen as the index building, following a real case. The structure is a dual system (hybrid) masonry infilled steel frame structure with 5-bays (transversal or y-direction) and 4-frames (longitudinal or x-direction). The lateral resisting system consists of concentric cross bracings in its transverse direction for all stories and a moment resisting frame in its longitudinal direction. Additional concentric cross bracings are also placed at the ground level (parking) on both directions. The building does not include any shear wall core, carrying the staircase load to act as a centre of stiffness.

The construction method and the structural arrangement are among the most common styles in middle-east region. The structure is assumed to be constructed in a highly seismic region, on semi-compact soil ($360\text{ m/s} < V_{s,30} < 800\text{ m/s}$). Hence, a peak ground acceleration of $0.35g$ and a soil type S_C (very dense soil and soft rock) according to UBC-97 has been employed for its design. An imposed load of 200 kg/m^2 and 150 kg/m^2 is considered for the floors and the roof (4th floor) respectively. The permanent load consists of floor finishing, joists and metal decks and is estimated equal to 350 kg/m^2 for the floors and 380 kg/m^2 for the roof (4th floor).

Fig. 4 illustrates the building plan of the first floor, indicating the location and dimensions of beams (IPE) columns (HEB) and bracings. All steel material used are S235 ($f_y=235\text{ MPa}$, $E=2.1 \times 10^5\text{ MPa}$, $\gamma=78\text{ kN/m}^3$) and the concrete slabs have a thickness of 0.15 cm with metal sheeting. The column sections are given in Table 1 and the beam sections are indicated along the elements in the building plan. For the bracings a hollow square section with a cross sectional area of $120 \times 120\text{ mm}^2$ has been implemented.

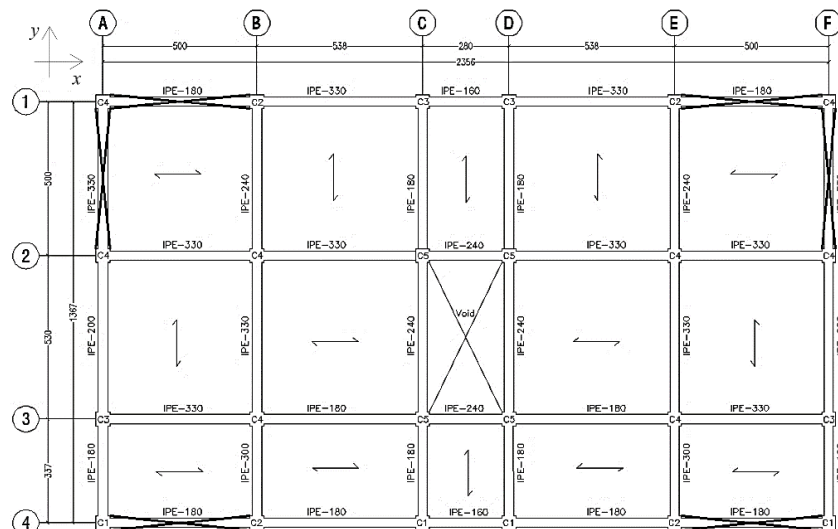


Fig. 4 - Plan of the 1st floor of the index building (units in centimetre)
IPE: European steel I-beam with parallel flange surfaces

Table 1 - Column sections used for the index building

HEB: European wide flange beams with parallel flange surfaces and approximate equal width and depth

Storey	C1	C2	C3	C4	C5
4 th	HEB-140	HEB-140	HEB-120	HEB-160	HEB-160
3 rd	HEB-140	HEB-140	HEB-120	HEB-160	HEB-160
2 nd	HEB-140	HEB-140	HEB-140	HEB-180	HEB-160
1 st	HEB-140	HEB-160	HEB-140	HEB-180	HEB-160

The building is modelled in three dimensions, using fibre based finite element software SeismoStruct [9]. The overall behaviour of the infill panels has been simulated following the equivalent strut approach, proposed by Crisafulli [10]. The hysteresis behaviour and mechanical properties of the panels were calibrated according to experimental studies on identical material used in construction of the index building. For instance, the infill panels were adjusted for solid clay bricks (219×110×66 mm) with no voids placed in running bond with Portland cement type I and sand mortar. A thorough discussion on the assumptions and the modelling process of the index building can be found in [11].

4.2 Nonlinear Dynamic Analysis

The seismic demand of the index building has been evaluated through incremental dynamic analysis [12]. As the nonlinear dynamic analysis is highly sensitive to the selection of ground motions, it is essential that the selected set of ground-motion records reflect the seismic hazard of the site under study and that the scaling of records is legitimate [13].

For this study, the far-field ground motion set based on the FEMA P695 has been selected. The suite of ground motions includes 22 record pairs, each with two horizontal components for a total of 44 ground motions. The records have a magnitude (M_w) range from 6.5 to 7.6 with an average magnitude of M_w 7.0 and all were recorded at sites located greater than or equal to 10 km from the fault rupture. Following the Eurocode 8 Soil classification, 16 sites are classified as stiff soil site and the remaining are classified as very stiff soil. In order to reduce the computational effort, only the component with highest peak ground acceleration has been employed, resulting in to 20 ground motions (Fig. 5). For IDA, each record was scaled to distinct spectral acceleration (S_a) levels, ranging from 0.1g to 2.5g with increments of 0.1g. The number and scaling of earthquake records, imply that 500 nonlinear dynamic runs were carried out at each critical stage of the index building. The IDA results, shown in Fig. 6, indicate the $S_a(T_1)$ versus maximum peak inter-storey drift ratio (MIDR) values for each scaling of individual records (grey circles) summarised into the 16th, 50th (median) and 84th fractiles.

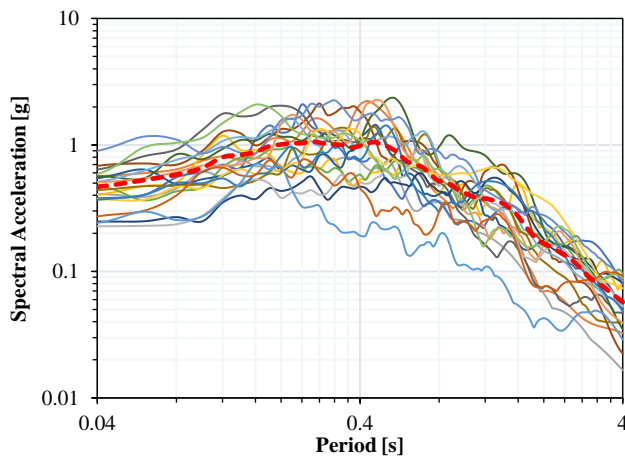


Fig. 5 - Response spectra of twenty individual components of the normalised far-field records of FEMA P695

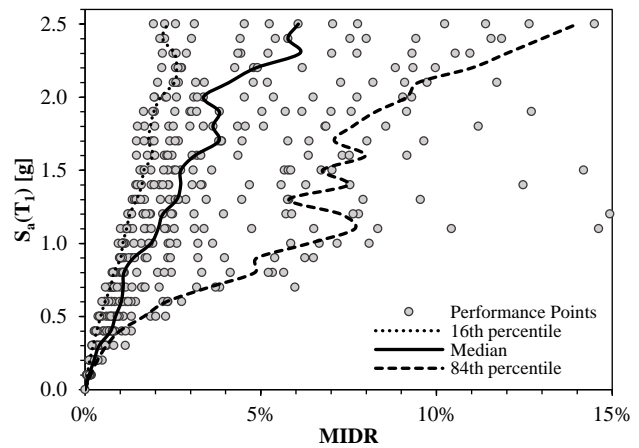


Fig. 6 - IDA results of the index building at its initial condition

It is thus an unavoidable fact that the IDA curves display large record-to-record variability, while the record scaling gives the opportunity to cover the entire range of structural response, from elasticity to yielding and finally collapse. The spectral shape of the mentioned ground motions was not a criterion in the selection process, as the

FEMA P695 far-field ground motion set are independent of site hazard or structural type. Therefore, the applied records are not reliant on period, nor the building-specific property of the structure and the hazard disaggregation.

4.3 Defining Damage Limit States

It is crucial to define rational damage limit states for deriving fragility curves of a structure. For this study, the damage states suggested by HAZUS-MH MR5 [14] and FEMA 356 [15] have been considered for characterising each of the limit-states. Furthermore, as the analysed building behaves as a composite structural system, where the initial lateral resistance is provided by the masonry infill walls, the applied damage thresholds should consider the contribution of masonry panels as well as the steel frame. Accordingly, four damage limit-states have been characterised for the overall damage of the building at various response levels as follows:

- 1) *Slight*: hairline cracks (diagonal or horizontal) appear on some of the infill walls; some bricks near the beam-column interaction start to break and crush.
- 2) *Moderate*: large cracks (diagonal or horizontal) on most infill walls; a number of bricks dislodged and fall; partial and full collapse of few walls; some walls may bulge out-of-plane; failure at some steel connections; some critical members may fail and the structure might undergo a permanent lateral deformation.
- 3) *Extensive*: total failure of many infill walls and loss of stability of steel frame; bracings and moment connections start to fail; some infill walls may bulge out-of-plane and consequently the structure loses its lateral resistance. Some steel frame connections may have failed. Structure may exhibit permanent lateral deformation or partial collapse due to failure of some critical members.
- 4) *Complete*: all infill panels disintegrate resulting in compression failure of the masonry struts and the steel frame has lost its stability completely, resulting in an imminent or immediate structural collapse.

To couple each damage state to its associated stage of structural behaviour, maximum peak inter-story drift ratio (MIDR) has been employed. Shear capacity can also be a good indicator of the damage in the infill panels; however, as the index building consists of steel frame and masonry panels, the selected EDP should be functional for both cases.

5. Life Cycle Cost Analysis

To estimate the expected life cycle cost, a scenario has been assumed for the 50-year life span of the index building. By applying progressive degradation (≈ 0.0016 capacity reduction per year) and sudden earthquake shocks (two events) the structural response have been monitored at any given time. The starting point of the curve (time zero), in which the structure is at its peak capacity is termed its initial condition. It was presumed that two seismic events with moment magnitudes ranging between 6.0 and 6.75, each having an annual rate of $\nu = 0.0132$, struck the building at 30th year (1st Event) and 45th year (2nd Event). Both deterioration effects can be measured in terms of ultimate capacity and MIDR, hence the total wear may be represented as a function of time as shown in Fig. 7.

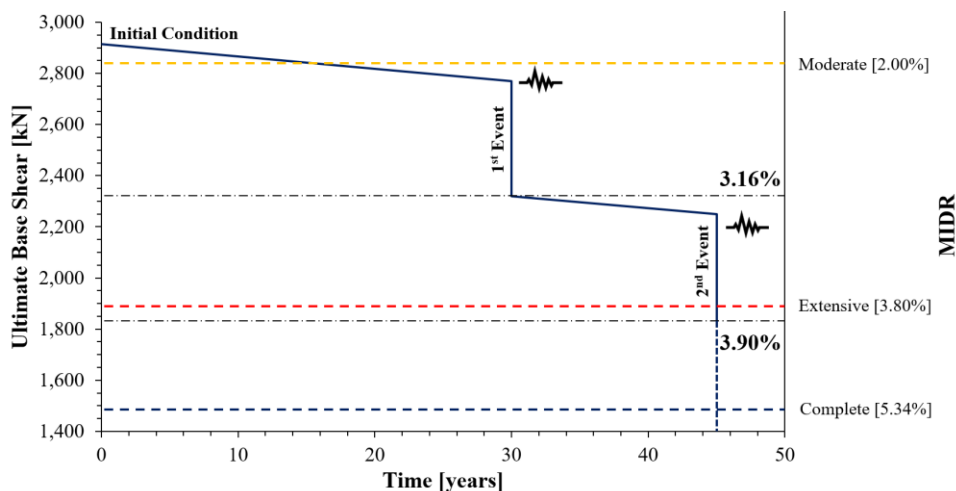


Fig. 7 – Design life of the index building subjected to aging and two earthquake events

The total life cycle cost (C_{Total}) of a structural system can be expressed as a function of the expected operating time period (e.g. $t = 50$ years) and design variable vectors (s) [16];

$$C_{Total}(t, s) = C_{IN}(s) + C_{LS}(t, s) \quad (7)$$

where C_{IN} is the initial cost of a new structure, including the material cost and the labour cost, right after the construction is finished, estimated as €150/m² for this case study. Since, the construction period is not considered in the model, C_{IN} is not time-dependent. The information regarding the cross sectional dimensions, the design load, resistance and material properties have all been accounted for in the design variable vector. The limit state dependent cost function $C_{LS}(t, s)$ considering N limit states can be estimated as follows;

$$C_{LS}(t, s) = \frac{v_E}{\lambda} (1 - e^{-\lambda t}) \sum_{i=1}^N C_{LS}^i P_i \quad (8)$$

$$P_i = P_i(\Delta > \Delta_i) - P_{i+1}(\Delta > \Delta_{i+1}) \quad (9)$$

where v_E is the annual occurrence rate of significant earthquakes ($M_w > 6.0$) modelled by Poisson process, which for the site under study is estimated as 0.0132. λ is the constant annual momentary discount rate selected as 2%, which aims to convert the cost due to hazard that occurs in the future into present euro value. The final life cycle cost is considerably sensitive to the discount value. C_{LS} is the limit-state dependent cost, referring to the potential damage cost from earthquake that may occur during the service life of the structure. The total life cycle cost can account for repair cost after an earthquake, the loss of contents cost, the cost of injury recovery or human fatality and other direct or indirect economic losses. As previously stated, P_i is the probability of the i^{th} limit state being violated, calculated using Eq. 6. The following will discuss the calculating process for each of the factors involved in the mentioned life cycle cost model.

The implementation of the LCC model requires the calculation of the annual probability of exceeding a limit-state given the occurrence rate of any earthquake intensity. Hence, the hazard curve of the region under study and the fragility curves of the structure at critical stages of its life span should be determined. The hazard curve demonstrated in Fig. 8, is obtained from the latest seismic hazard analysis of the site. Due to structural deterioration and its consequential stiffness decay, the fundamental period (T_1) of the structure increases with time. The variation of structural frequency influences the applied value of the hazard as well. Although, this impact is minor, it has been included in the model calculations.

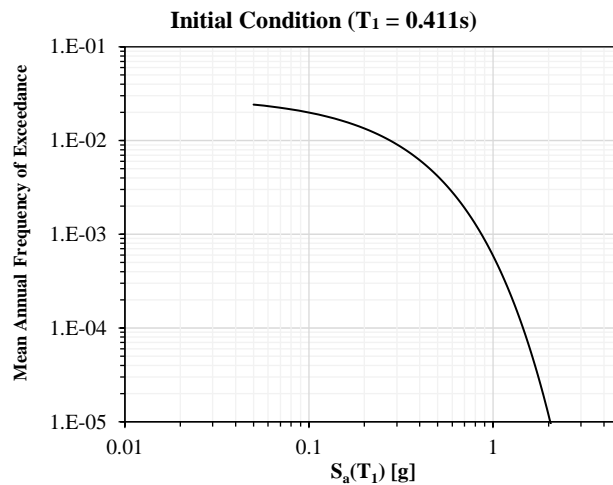


Fig. 8 – Hazard curve of the structure at its initial condition located on soft rock ($V_{s,30} = 525$ m/s)

The analytical fragility functions are derived for each of the three main stages of the building's life span. The curves are obtained by fitting a parametric model to the performance points obtained from IDA analysis. Since there are no directivity-influenced records in the earthquake suite and the selected building is mid height (i.e. first-mode-dominated) the spectral pseudo-acceleration corresponding to the first-mode elastic vibration period ($S_a(T_1)$)

and 5% damping ratio is chosen to characterise the intensity of earthquakes (IM). Furthermore, as previously mentioned, the maximum peak inter-story drift ratio (MIDR) has been adopted to represent the engineering demand parameter (EDP).

The MIDR values used as damage thresholds for the fragility analysis are given in Table 2. For this purpose, exceedance of the selected damage index from the corresponding value associated with each of these performance levels, indicates the fragility of the system in that specific performance level.

Table 2 – Maximum peak inter-story drift ratio values assigned to different damage states at each critical stage of the building’s life

Damage Limit State	Initial Condition	1 st Event	2 nd Event
<i>Slight</i>	0.43%	0.45%	0.28%
<i>Moderate</i>	2.00%	1.54%	0.89%
<i>Extensive</i>	3.80%	2.61%	2.21%
<i>Complete</i>	5.34%	3.96%	3.27%

Fig. 9 illustrates the static pushover curves and the assigned damage thresholds, corresponding to each critical stage of the index building.

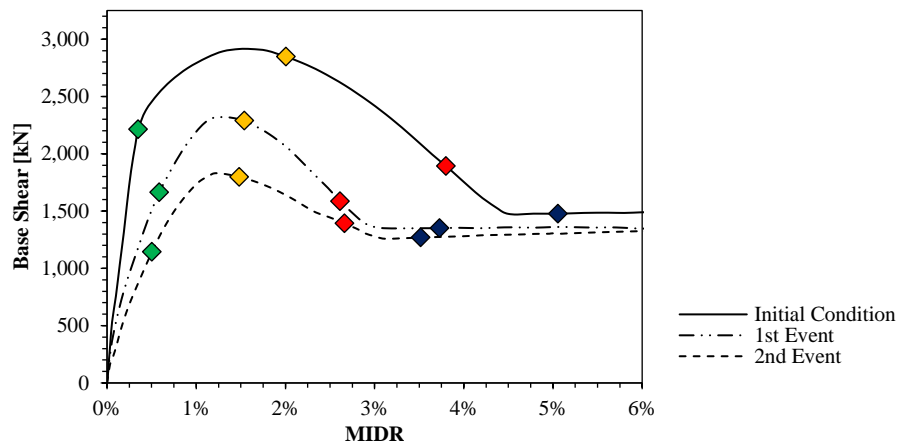


Fig. 9 - Pushover curves of index structure at each critical stage and the corresponding damage thresholds

The generalised linear model (GLM) has been implemented for developing fragility curves. GLMs are a variation of ordinary linear regression, in which the predictor variables are linearly related to response via a link function $g(\cdot)$. In this case a complementary log-log link function is adapted. The probability of exceeding a particular damage state threshold (ds_i) given the IM value can be expressed as follow:

$$P(DS \geq ds_i | IM) = g(\mu)^{-1} (\alpha + \beta \log (IM)) \tag{10}$$

$$g(\mu) = \log (-\log(1 - \mu)) \tag{11}$$

The median (μ) and dispersion (β) (i.e. standard deviation of $\ln(IM)$) obtained for each fragility curve are given in Table 3. The fragility curves derived for each critical stage of the structure are presented in Fig. 10.

Table 3 - Median (μ) [g] and Dispersion (β) values

Damage Limit State	Initial Condition		1 st Event		2 nd Event	
	μ	β	μ	β	μ	β
<i>Slight</i>	0.315	0.323	0.296	0.469	0.203	0.397
<i>Moderate</i>	1.021	0.507	0.766	0.552	0.446	0.555
<i>Extreme</i>	1.554	0.573	1.104	0.671	0.923	0.601
<i>Complete</i>	1.793	0.622	1.351	0.589	1.090	0.604

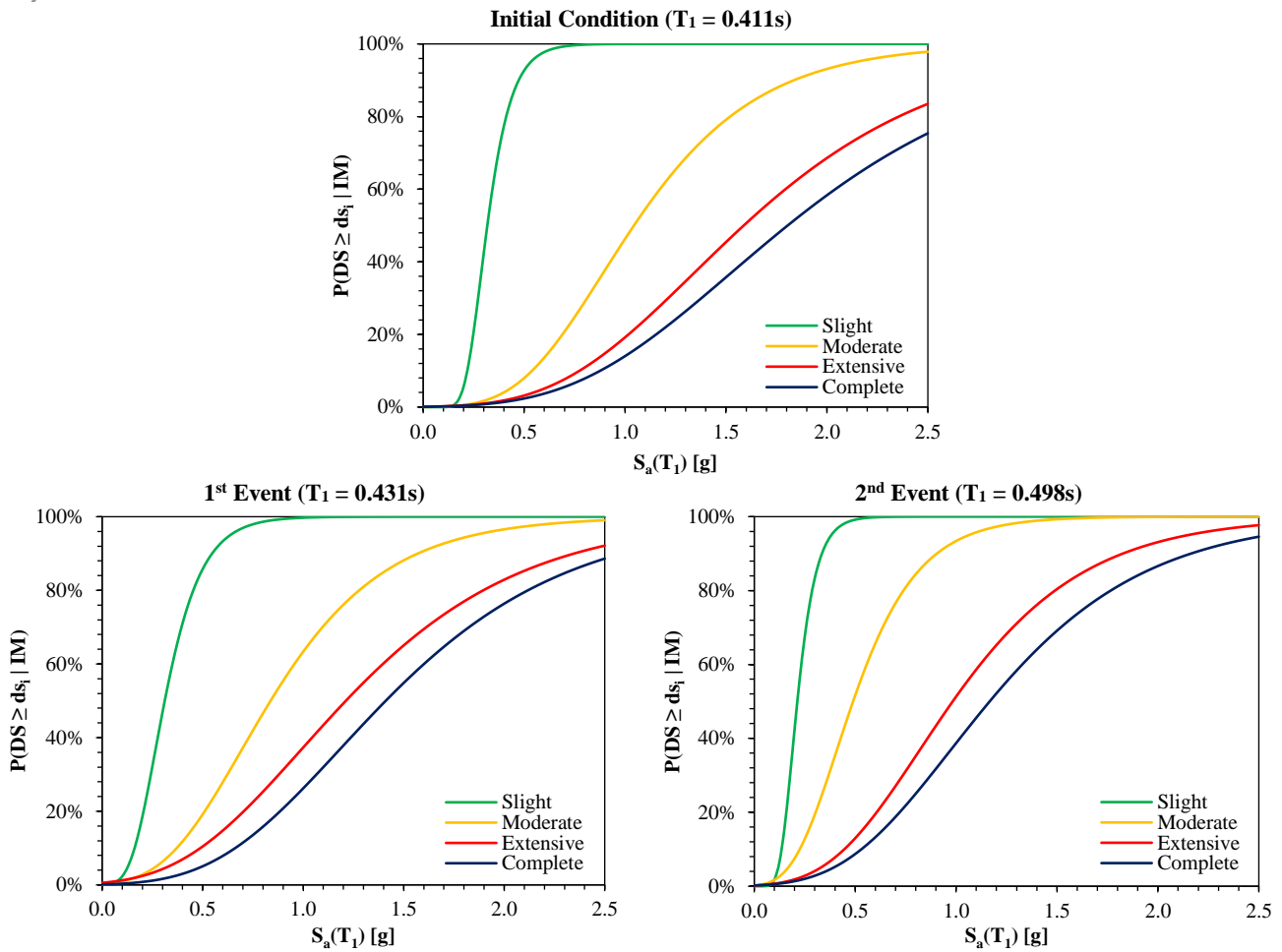


Fig. 10 – Fragility curves of index structure at each critical stage of the building’s life span

In order to estimate the limit-state dependent cost function $C_{LS}(t, s)$ the probability of any given limit state being violated $P_i(\Delta > \Delta_i)$ given the earthquake occurrence $\Delta\lambda_{IM}(x_i)$ should be calculated using Eq. 6. The earthquake occurrence at each of the considered stages were determined using the hazard curves corresponding to the structure’s initial period (T_1). The probability of exceeding each of the defined damage stages during the operational life span of the structure are shown in Fig. 11.

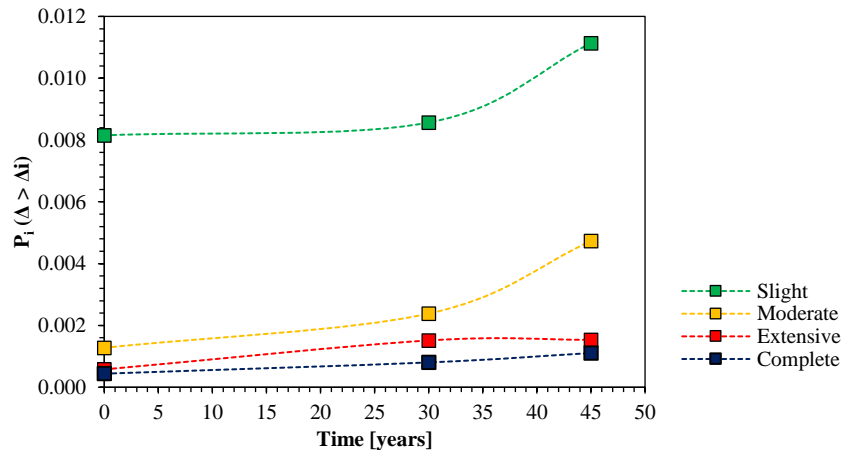


Fig. 11 - Probability of exceeding different damage states, given the earthquake occurrence at each stage of the building’s life span

The limit-state dependent cost (C_{LS}) for the i^{th} limit-state can be expressed as follows:

$$C_{LS}^i = C_{dam}^i + C_{con}^i + C_{ren}^i + C_{inc}^i + C_{rel}^i + C_{inj,m}^i + C_{inj,s}^i + C_{fat}^i \quad (12)$$

The description and calculation details for each of the cost components according to the location under study are presented in Table 4. An occupancy rate of three persons per each unit (65 m² / 2 bedrooms) has been considered based on the social function classification data [17]. Seismic damage may render the performance of the structure from its normal functions until repairs or complete replacement is executed. Rents and other incomes may be suspended during this period and relocation cost may also be incurred. In this study, the cost of relocation has not been included. The economic losses can be divided into two factors, rental and income. The studied building is residential only and no disruption will be exerted on the commercial activities. The rental cost loss is expected to be proportional to duration of complete or partial loss function. Furthermore, the values allocated for injuries and fatalities are based on typical insurance provided in the region under study.

Table 4 – Limit-state cost components

Variable	Cost Category	Calculation Formula	Basic Cost
C_{dam}^i	Damage/Repair	Replacement Cost × Floor Area (1'340 m ²) × Mean Damage Index	Replacement: €150/m ²
C_{con}^i	Loss of Contents	Unit Contents Cost × Floor Area (1'340 m ²) × Mean Damage Index	Contents: €50/m ²
C_{ren}^i	Rental	Rental Rate (€300/month) × Gross Leasable Area (764 m ²) × Loss of Function	Rent: €4.6/month/m ²
C_{inc}^i	Income	Rental Rate × Gross Leasable Area (764 m ²) × Down Time	-
C_{rel}^i	Relocation	Relocation Cost × Gross Leasable Area (764 m ²) × Loss of Time	-
C_{inj}^i	Injury	Injury Cost Per Person × Expected Injury Rate	Minor: €5'000/person Serious: €50'000/person
C_{fat}^i	Human Fatality	Death Cost Per Person × Expected Death Rate	€2'500'000/person

The mean damage indices are selected according to the central values proposed in FEMA 227 [17] and Risk-UE [18]. Two cases corresponding to Total I and Total II been considered, where the limit-state dependent cost with and without considering injury and death cost is calculated respectively (Table 5).

Table 5 – Detail of limit-state dependent cost [all values in Euro € currency]

Limit State	Damage/Repair	Loss of Contents	Rental	Minor Injury	Serious Injury	Human Fatality	Total I	Total II
No Damage	0	0	0	0	0	0	0	0
Slight	3,015,000	1,005,000	33,387	110	1,100	18,500	4,073,097	4,053,387
Moderate	9,045,000	3,015,000	122,407	1,750	17,500	225,000	12,426,657	12,182,407
Extensive	16,080,000	5,360,000	229,877	17,850	178,500	2,250,000	24,116,227	21,669,877
Complete	20,100,000	6,700,000	351,440	179,750	1,797,500	44,975,000	74,103,690	27,151,440

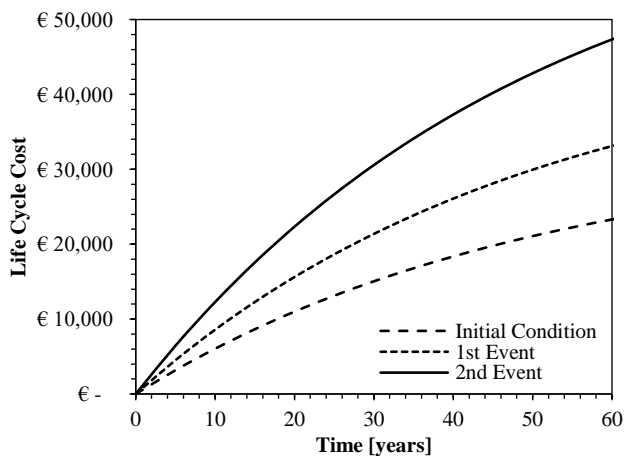


Fig. 12 – Expected life cycle cost at each critical stage

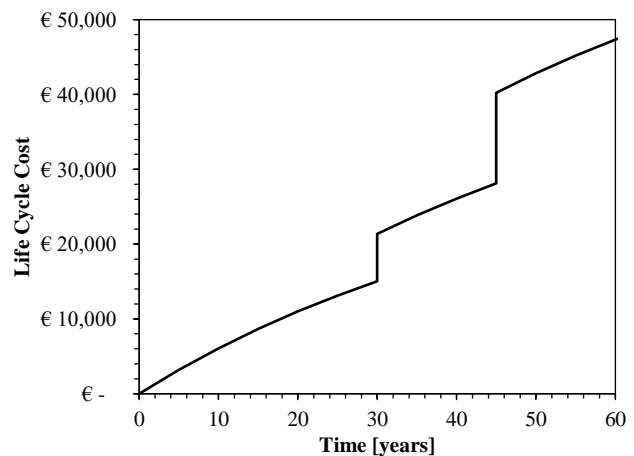


Fig. 13 – Total expected life cycle cost (Total II)



A parametric study was conducted for each critical stage to investigate the variation of the limit-state dependent cost throughout the building's lifetime (Fig. 12). The service life of the structure is only considered up to 60 years, since after passing this period the structure can be categorised as a historical building and hence the economic model needs to be changed. The expected life cycle of the structure, following the assumed scenario, is shown in Fig. 13. In this case, the limit-state dependent cost does not include the cost of injury or fatality and for simplicity the initial cost of the structure has not been included.

6. Conclusion

The life cycle cost of a residential, mid-rise infilled steel frame structure has been estimated, while considering a scenario for its initial 50-year life span. The effect of both continues progressive deterioration and extreme sudden events have been included in the analysis. Two earthquake events were assumed to occur throughout the building's life span, each capable of causing considerable damage to the structure. The performance of the structure was investigated by means of incremental dynamic analysis at the building's initial condition and following the occurrence of each extreme event. Accordingly, the analytical fragility curves were derived for each of the critical stages and later employed in the LCC model. By calculating the limit-state dependent cost $C_{LS}(t, s)$ for each of the studied stages, the total life cycle cost for the assumed scenario was estimated. It was found that the LCC model is highly sensitive to the constant annual momentary discount rate (λ). Moreover, the sensitivity of the results indicates the importance of accurate estimation of structural vulnerability and detailed regional hazard assessment. Having a rational forecast of structure's LCC can assist in financial resource allocation and management for both pre- and post- disaster. Furthermore, the predicted structural behaviour at each stage of the building's operational life can specify the most appropriate precautionary strategies to consider and follow.

7. References

- [1] Sanchez-Silva M, Klutke GA, Rosowsky DV (2011): Life Cycle Performance of Structures Subject to Multiple Deterioration Mechanisms. *Structural Safety*, Volume 33, Issue 3, pp.206–217.
- [2] Bastidas E, Sanchez-Silva M, Chateneuf A, Ribas Silva M (2007): Coupled Reliability Model of Biodeterioration, Chloride Ingress and Cracking for Reinforced Concrete Structures. *Structural Safety*, Volume 30, Issue 2, pp.110–129.
- [3] Bastidas E, Bressolette P, Chateneuf A, Sánchez-Silva M (2009): Probabilistic Lifetime Assessment of RC Structures Under Coupled Corrosion–Fatigue Deterioration Processes. *Structural Safety*, Volume 31, Issue 1, pp.84–96.
- [4] Rao A, Lepech M, Kiremidjian A, Sun XY (2010): Time Varying Risk Modeling of Deteriorating Bridge Infrastructure for Sustainable Infrastructure Design. *5th International Conference On Bridge Maintenance Safety Management and Life Cycle Optimization*, CRC Press, Taylor & Francis Group.
- [5] Frangopol DM, Kallen M-J, Van Noortwijk JM (2004): Probabilistic Models for Life Cycle Performance of Deteriorating Structures: Review and Future Directions. *Progress in Structural Engineering and Material*, Volume 6, Issue 4, pp.197–212.
- [6] Giorgio M, Guida M, Pulcini G (2011): An Age- And State-Dependent Markov Model for Degradation Processes. *IIE Transactions*, Volume 43, Issue 9, pp.621–632.
- [7] Iervolino I, Giorgio M, Chioccarelli E (2013): Gamma Degradation Models for Earthquake-Resistant Structures. *Structural Safety*, Volume 45, pp.48–58.
- [8] McGuire RK (2004): Seismic Hazard and Risk Analysis. *Earthquake Engineering Research Institute*, Oakland, CA. pp.178.
- [9] Seismosoft (2013): SeismoStruct v7.0, A Computer Program for Static and Dynamic Nonlinear Analysis of Framed Structures.
- [10] Crisafulli FJ, Carr AJ (2007): Proposed Macro-Model for The Analysis of Infilled Frame Structures. *Bulletin of the New Zealand Society for Earthquake Engineering*, Volume 40, No 2.
- [11] Nassirpour A, D' Ayala D (2014): Fragility Analysis of Mid-Rise Masonry Infilled Steel Frame (MISF) Structures. *Second European Conference on Earthquake Engineering and Seismology*, Istanbul, Turkey.
- [12] Vamvatsikos D, Cornell CA (2002): Incremental Dynamic Analysis. *Earthquake Engineering & Structural Dynamics*, Volume 31, Issue 3, pp.491–514.
- [13] Baker JW, Cornell AC (2006): Spectral Shape, Epsilon and Record Selection. *Earthquake Engineering & Structural Dynamics*, Volume 35, Issue 9, pp.1077–1095.
- [14] HAZUS-MH MR5 (2013): Advanced Engineering Building Module (AEBM) - Technical and User's Manual. *Federal Emergency Management Agency*, Washington D.C.
- [15] FEMA 356 (2000): Pre-Standard and Commentary for The Seismic Rehabilitation of Buildings. *Federal Emergency Management Agency*, Washington D.C.
- [16] Wen YK, Kang YJ (2001): Minimum Building Life Cycle Cost Design Criteria. I: Methodology. *Journal of Structural Engineering*, Volume 127, Issue 3, pp.330–337.
- [17] FEMA 227 (1992): A Benefit-Cost Model for The Seismic Rehabilitation of Buildings. *Federal Emergency Management Agency*, Vols. I & II.
- [18] Mouroux P, Le Brun B (2006): RISK-UE an Advanced Approach to Earthquake Risk Scenarios with Applications to Different European Town. Final Report. *European Commission*, Brussels.